Hindawi
Complexity
Volume 2018, Article ID 2381568, 9 pages
https://doi.org/10.1155/2018/2381568

*Research Article*

# Modelling and Analysis of Automobile Vibration System Based on Fuzzy Theory under Different Road Excitation Information

**Xue-wen Chen and Yue Zhou**

*College of Automobile and Traffic Engineering, Liaoning University of Technology, Jinzhou 121001, China*

Correspondence should be addressed to Xue-wen Chen; xuewen.chen@163.com

Received 16 May 2017; Revised 23 June 2017; Accepted 6 November 2017; Published 2 January 2018

Academic Editor: Sigurdur F. Hafstein



A fuzzy increment controller is designed aimed at the vibration system of automobile active suspension with seven degrees of freedom (DOF). For decreasing vibration, an active control force is acquired by created Proportion-Integration-Differentiation (PID) controller. The controller's parameters are adjusted by a fuzzy increment controller with self-modifying parameters functions, which adopts the deviation and its rate of change of the body's vertical vibration velocity and the desired value in the position of the front and rear suspension as the input variables based on 49 fuzzy control rules. Adopting Simulink, the fuzzy increment controller is validated under different road excitation, such as the white noise input with four-wheel correlation in time-domain, the sinusoidal input, and the pulse input of C-grade road surface. The simulation results show that the proposed controller can reduce obviously the vehicle vibration compared to other independent control types in performance indexes, such as, the root mean square value of the body's vertical vibration acceleration, pitching, and rolling angular acceleration.

## 1. Introduction

It is generally known that automobile active suspension system can produce and adjust the active control force in time to restrain the vehicle body's vibration for improving the ride comfort according to the road surface excitation. Recently, there have been large research achievements in the automobile suspension system, such as the optimization control theory, the PID theory, the theory of variable structure control, and the skyhook damping theory which have been applied generally to the vibration control system. Zhang et al. proposed a semiactive suspension controller with magnetorheological dampers to realize independent control based on modified skyhook damping scheme of quarter-vehicle subsuspension system in the full vehicle [1]. Ren et al. presented an adaptive hybrid control algorithm combined with the ground-hook and skyhook control strategies based on quarter car model of semiactive suspension and designed an unscented Kalman filter to estimate the suspension states [2]. Singh and Aggarwal designed a hybrid Fuzzy-PID controller to evaluate the passenger ride comfort based on a semiactive quarter car model having MR shock absorber [3]. Du et al. presented an approach in designing a robust controller for half-car model active suspensions considering changes in vehicle inertial properties, such as the suspension deflection limitation and the controller saturation problem [4]. Owing to the randomness of road surface roughness and the nonlinearity and uncertainty of vehicle system, the above-mentioned method has its disadvantages and adaptability [5–7]. It has been known that the intelligent control theory has the ability of logical reasoning and decision-making, and it is best suited to solve the complexity and uncertainty system [8–10]. Therefore, a variety of intelligent control methods has been widely used like the fuzzy control, neural network, genetic algorithm, and so on [11–14]. Huang et al. designed a fuzzy controller for converting chaos into periodic motion of stable performance based on the neural-net tyre model [10]. Riaz et al. presented adaptive Neuro Fuzzy Takagi-Sugeno-Kang control strategies for the vehicle active suspension to improve the ride quality and vehicle stability [13]. Zirkohi and Lin proposed an interval type-2 fuzzy-neural network approach incorporating the Lyapunov design approach and SMC method to improve controller robustness [14]. Balamurugan et al. designed two controllers

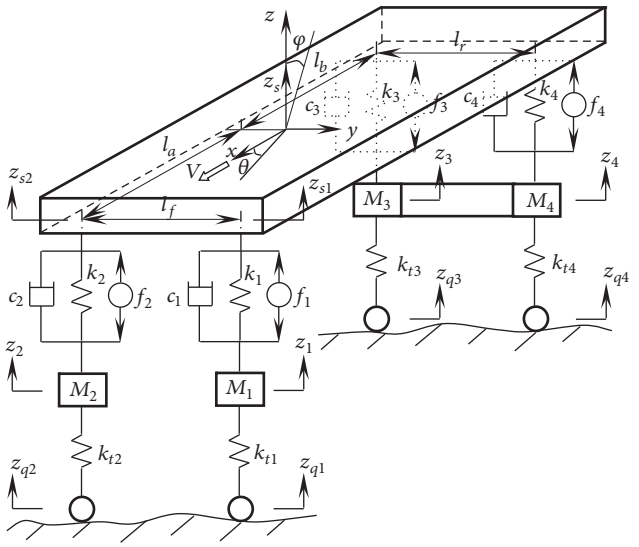


Figure 1: Vehicle model of the active suspension with seven DOF.

to generate the desired damping force and adjust the voltage level to MR damper based on the quarter car vehicle model of semiactive suspension [15]. Zhang et al. designed a semiactive controller based on the inverse model and sliding mode control strategies for the quarter-vehicle suspension with the magnetorheological damper [16]. Bououden et al. investigated the problem of time-varying delays and input constraints for active suspension systems with a quarter-vehicle model based on the Lyapunov-Krasovskii method [17]. From the analysis results on automobile active suspension research, we learned that much of the relevant literature focus on a quarter- or a half-car model that cannot fully reflect or evaluate riding comfort of a whole vehicle [18–22]. So, it is our goal to research the time-domain response of the automobile active suspension with seven DOF for decreasing the body vibration considering the pitching and rolling motion under the condition of the white noise input with four wheels correlated effects and different road excitation. At last, the submodule of fuzzy increment controller and the random input model have been given, and the effectiveness of proposed controller has been validated adopting Simulink.

## 2. Vehicle Vibration Model of the Active Suspension with Seven DOF

*2.1. Dynamic Model of Active Suspension.* Figure 1 describes a vehicle vibration model of the active suspension with seven DOF, including the body's vertical motion, pitching and rolling motion, and four vertical motions of the unsprung mass.

In Figure 1, $M_s$ represents the sprung mass; $M_1$, $M_2$, $M_4$, and $M_3$ represent the mass between the front and rear wheels on left and right sides, respectively. $z_s$ denotes the vertical displacement of the body center of mass (7); $\theta$ and $\varphi$ denote the pitch and roll angle displacement. $z_{s1}$, $z_{s2}$, $z_{s4}$, and $z_{s3}$ represent the body vertical displacement in position of the front and rear suspension on left and right sides, respectively. $z_1$, $z_2$, $z_4$, and $z_3$ represent the vertical displacement in position of the front and rear wheel on left and right sides, respectively. $z_{q1}$, $z_{q2}$, $z_{q4}$, and $z_{q3}$ represent the road irregularity excitation, respectively. $k_1$, $k_2$, $k_4$, and $k_3$ represent the elastic stiffness of the front and the rear suspension. $k_{t1}$, $k_{t2}$, $k_{t4}$, and $k_{t3}$ represent the elastic stiffness of the front and rear wheel on left and right sides, respectively. $c_1$, $c_2$, $c_4$, and $c_3$ represent the damping of the front and rear suspension, respectively. $f_1$, $f_2$, $f_4$, and $f_3$ represent the control force from the active controller in position of the front and rear suspension on left and right sides, respectively. $l_a$ and $l_b$ denote the distance of front and rear axle to the body center of mass. $l_f$, $l_r$ denote the distance between the left and right wheel. $V$ represents the vehicle's driving direction.

*2.2. Dynamic Differential Equation.* According to the vehicle vibration model of the active suspension, the dynamic differential equations with seven DOF are derived as follows.

The dynamic differential equation of the body's vertical motion is listed as follows:

$$M_s\ddot{z}_s + \sum_{i=1}^{4} F_i = 0 \quad (i = 1, \ldots, 4). \tag{1}$$

The dynamic differential equation of the body's pitch motion is listed as follows:

$$I_y\ddot{\theta} - (F_1 + F_2)\cdot l_a + (F_3 + F_4)\cdot l_b = 0. \tag{2}$$

The dynamic differential equation of the body's roll motion is listed as follows:

$$I_x\ddot{\varphi} + (F_2 - F_1)\cdot \frac{l_f}{2} + (F_3 - F_4)\cdot \frac{l_r}{2} = 0. \tag{3}$$

The dynamic differential equation of the vertical motion of four unsprung mass is listed as shown in equation (3).

$$M_i\ddot{z}_i - F_i + k_{ti}(z_i - z_{qi}) = 0 \quad (i = 1, \ldots, 4), \tag{4}$$

where $F_i$ from (1) to (4) is expressed as

$$F_i = c_i(\dot{z}_{si} - \dot{z}_i) + k_i(z_{si} - z_i) - f_i \quad (i = 1, \ldots, 4). \tag{5}$$

Here, $\dot{z}_{si}$ is listed as follows:

$$\begin{aligned} z_{s1} &= z_s - l_a\theta - \frac{\varphi l_f}{2};\\ z_{s2} &= z_s - l_a\theta + \frac{\varphi l_f}{2}\\ z_{s3} &= z_s + l_b\theta + \frac{\varphi l_r}{2};\\ z_{s4} &= z_s + l_b\theta - \frac{\varphi l_r}{2}. \end{aligned} \tag{6}$$

In the above expression, $\ddot{z}_s$, $\ddot{\theta}$, and $\ddot{\varphi}$ represent the vertical vibration and the pitch and roll angle acceleration of the body center of mass, respectively. $\ddot{z}_1$, $\ddot{z}_2$, $\ddot{z}_4$, and $\ddot{z}_3$ represent the

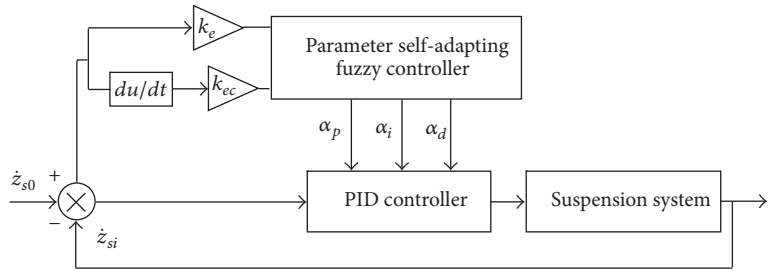


Figure 2: Principle diagram of the Fuzzy-PID controller.

vertical vibration and the pitch and roll angle acceleration in position of the front and rear wheel on left and right sides, respectively. $\dot{z}_1$, $\dot{z}_2$, $\dot{z}_4$, and $\dot{z}_3$ represent the vertical vibration velocity in position of the front and rear wheel on left and right sides, respectively. $\dot{z}_{s1}$, $\dot{z}_{s2}$, $\dot{z}_{s4}$, and $\dot{z}_{s3}$ represent the vertical vibration velocity in position of the front and rear suspension on left and right sides, respectively. $\ddot{z}_s$ denotes the vertical vibration velocity of the body center of mass. $I_x$ and $I_y$ represent the rotary inertia about the $x$ and $y$ axis, respectively.

## 3. Design of the Fuzzy Increment Controller of Automobile Active Suspension

*3.1. Fuzzy Controller Design.* The fuzzy increment controller includes two parts, the parameter self-adapting fuzzy controller and the PID controller, where the fuzzy controller adopts the deviation and its rate of change of the body vertical vibration velocity ($\dot{z}_{si}$) and the desired value ($\dot{z}_{s0}$) in the position of the front and rear suspension is the input variables; the increments ($\Delta K_p$, $\Delta K_i$, and $\Delta K_d$) of the PID controller parameters ($K_p$, $K_i$, and $K_d$) are derived according to a fuzzy control rule. The working principle of fuzzy increment controller is as shown in Figure 2.

$$\begin{aligned} K_p' &= K_p + \alpha_p \cdot \Delta K_p \\ K_i' &= K_i + \alpha_i \cdot \Delta K_i \\ K_d' &= K_d + \alpha_d \cdot \Delta K_d, \end{aligned} \tag{7}$$

where $k_e$ and $k_{ec}$ represent the conversion factor from the exact value to the fuzzy variable. $\alpha_p$, $\alpha_i$, and $\alpha_d$ represent the modified coefficient of the increments value of the PID controller parameters.

*3.1.1. Fuzzification of Input and Output Variable.* The input variable of the parameter self-adapting fuzzy controller ($\dot{z}_{si}$ and $\ddot{z}_{si}$ ($i = 1, \ldots, 4$)) and the output variable of the controller ($\Delta K_p$, $\Delta K_i$, and $\Delta K_d$) are described by the following seven fuzzy language variables, such as NB (Negative Big), NM (Negative Middle), NS (Negative Small), ZO (Zero), PS (Positive Small), PM (Positive Middle), and PB (Positive Big). Here, the domain ranges of the input variable ($\dot{z}_{si}$ and $\ddot{z}_{si}$) and the output variable ($\Delta K_p$, $\Delta K_i$, and $\Delta K_d$) are between −3 and 3, and between −1 and 1, respectively. The membership functions of all the variables are similar and as shown in Figure 3.

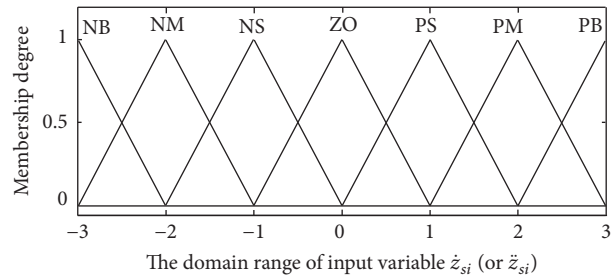


Figure 3: The membership functions of the input variable.

*3.1.2. Construct Rule Base.* Table 1 describes the relation between the input and output variable, where the fuzzy control rules are characterized by If-Then statements involving fuzzy linguistic variables. For example, the generic form of the fuzzy rules in the case of MIMO is as follows:

> If $x$ is $A_i$, . . ., and $y$ is $B_i$, Then $z$ is $C_i$, $k$ is $D_i$, $m$ is $E_i$, $i = 1, 2, \ldots, n$

For Table 1, if the deviation of the body vertical vibration velocity ($\dot{z}_{si}$) is NB, and the change rate of the velocity deviation ($\ddot{z}_{si}$) is NB, then the output variable $\Delta K_p$ is PB, $\Delta K_i$ is NB, and $\Delta K_d$ is PS.

*3.1.3. Defuzzification.* The defuzzifier is utilized to yield a nonfuzzy decision or control action from an inferred fuzzy control action by the fuzzy reasoner. The method on the center of Gravity is used to calculate the defuzzified output as follows: $U = \sum_{i=1}^{N} \omega_i u_i / \sum_{i=1}^{N} \omega_i$, where $N$ is the number of fuzzy rules, $u_i$ is the output of fuzzy rule base, and $w_i$ is the weight of $u_i$.

*3.2. PID Controller Design.* Adopting the deviation of vertical vibration velocity ($\dot{z}_{si}$) and its desired value ($\dot{z}_{s0}$) in the position of the front and rear suspension as the input variables of the PID controller in the Figure 2, an active control force ($f_i$ ($i = 1, \ldots, 4$)) is obtained as shown in

$$f(t) = K_p e(t) + K_i \int_0^t e(t)\, dt + K_d \frac{de(t)}{dt}, \tag{8}$$

Table 1: Fuzzy control rule of the PID increment parameters.

| $\Delta K_p$ / $\Delta K_i$ / $\Delta K_d$ | $\ddot{z}_{si}$ | | | | | | |
|---|---|---|---|---|---|---|---|
| $\dot{z}_{si}$ | NB | NM | NS | ZE | PS | PM | PB |
| NB | PB | PB | PM | PM | PS | ZE | ZE |
| | NB | NB | NM | NM | NS | ZE | ZE |
| | PS | NS | NB | NB | NB | NM | PS |
| NM | PB | PB | PM | PS | PS | ZE | NS |
| | NB | NB | NM | NS | NS | ZE | ZE |
| | PS | NS | NM | NM | NM | NS | ZE |
| NS | PM | PM | PM | PS | ZE | NS | NS |
| | NB | NM | NS | NS | ZE | PS | PS |
| | ZE | NS | NM | NM | NS | NS | ZE |
| ZE | PM | PM | PS | ZE | NS | NM | NM |
| | NM | NM | NS | ZE | PS | PM | PM |
| | ZE | NS | NS | NS | NS | NS | ZE |
| PS | PS | PS | ZE | NS | NS | NM | NM |
| | NM | NS | ZE | PS | PS | PM | PM |
| | ZE | ZE | ZE | ZE | ZE | ZE | ZE |
| PM | PS | ZE | NS | NM | NM | NM | NB |
| | ZE | ZE | PS | PS | PM | PB | PB |
| | PM | NS | PS | PS | PS | PS | PB |
| PB | ZE | ZE | NM | NM | NM | NB | NB |
| | ZE | ZE | PS | PM | PM | PB | PB |
| | PB | PM | PM | PM | PS | PS | PB |

where $K_p$, $K_i$, and $K_d$ represent the gain coefficient of the proportion, integral, and differential. The $e(t)$ denotes a deviation between the body vertical vibration velocity ($\dot{z}_{si}$) and its desired value ($\dot{z}_{s0}$ is set to zero). Here, $K_p = 3000$, $K_i = 20$, and $K_d = 30$.

## 4. Simulation

*4.1. Modelling Road Input Excitation with Four-Wheel Correlation in Time-Domain.* In order to validate the effectiveness of fuzzy increment controller, the white noise random input with four wheels correlated in time-domain, the sinusoidal input, and the pulse input of C-grade road surface are adopted, respectively. Here, the white noise random input on the left front wheel is shown as

$$\dot{Z}_{q1}(t) = -2\pi v f_0 Z_q(t) + 2\pi n_0 \sqrt{G_q(n_0)}\, v w(t), \quad (9)$$

where $n_0$ denotes a referenced spatial frequency and the value equals 0.1 ($m^{-1}$). $G_q(n_0)$ equals $256 \times 10^{-6}$ ($m^2/m^{-1}$) and it denotes a road roughness coefficient of C-grade road surface. $w(t)$ represents a white noise with mean zero. $v$ denotes the vehicle speed ($v = 20$ m/s) and $f_0$ equals 0.01.

Considering the delay effect, the random input on the left rear wheel is denoted as $\dot{Z}_{q4}(t) = \dot{Z}_{q1}(t - \tau)$. Here, $\tau = L/v$ and $L$ represents wheelbase. So, the random input on the left rear wheel is expressed as

$$\dot{Z}_{q4}(t) = -\dot{Z}_{q1}(t) + \frac{2vZ_{q1}(t)}{L} - \frac{2vZ_{q4}(t)}{L}. \quad (10)$$

According to the early literatures, the random input on the right front wheel is derived as

$$\dot{Z}_{q2}(t) = \dot{Z}_{q1}(t) - \frac{12vZ_{q1}(t)}{B} + x_2. \quad (11)$$

Also, the random input on the right rear wheel is denoted as $\dot{Z}_{q3}(t) = \dot{Z}_{q2}(t - \tau)$. Therefore, the random input on the right rear wheel is calculated as

$$\dot{Z}_{q3}(t) = -\dot{Z}_{q2}(t) + \frac{2vZ_{q2}(t)}{L} - \frac{2vZ_{q3}(t)}{L}, \quad (12)$$

where

$$\dot{x}_1 = -\frac{12vZ_{q1}(t)}{B} + x_2,$$
$$\dot{x}_2 = \frac{72v^2Z_{q1}(t)}{B^2} - \frac{12v^2x_1}{B^2} - \frac{6vx_2}{B}. \quad (13)$$

In formula (10) and formula (11), $B$ denotes the lateral distance between the left and right wheel, $L$ represents the longitudinal distance between the front and rear wheel (i.e., the wheelbase), and $v$ is car speed at the moment.

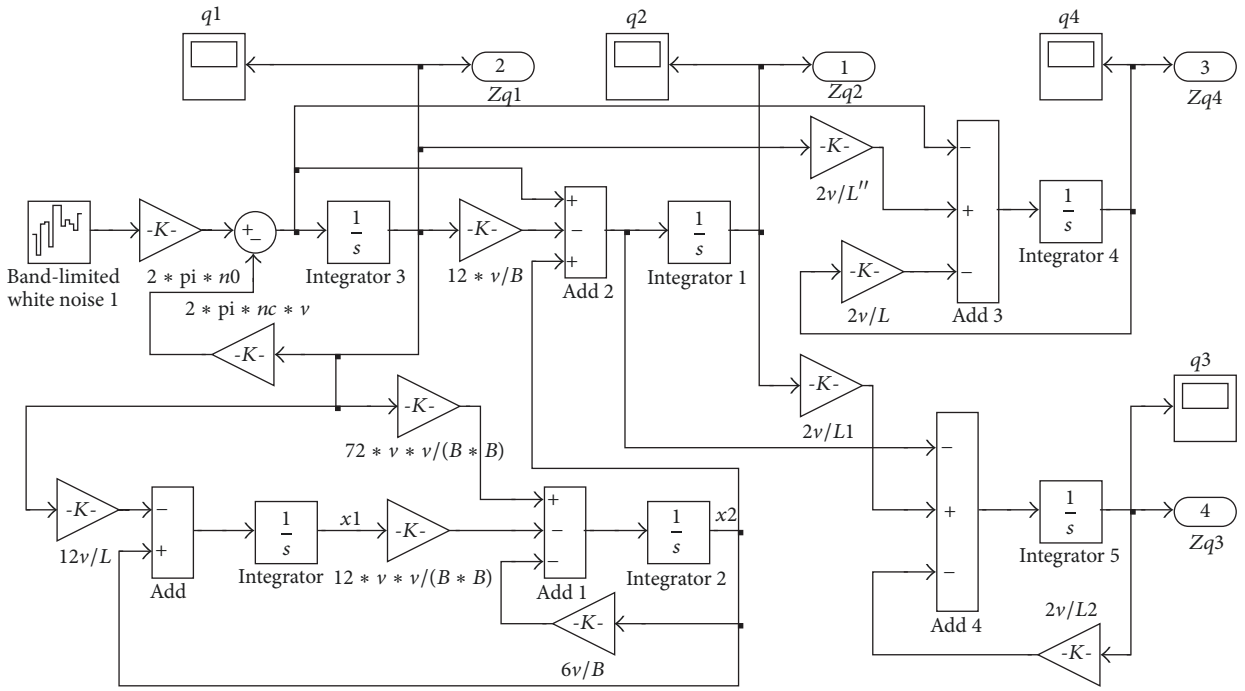


Figure 4: Random input model with four-wheel correlation in time-domain.

Table 2: Suspension structure parameters of a test car.

| Variable | Value | Dimension |
|---|---|---|
| $M_s$ | 770 | kg |
| $M_1$ $M_2$ | 35 | kg |
| $M_3$ $M_4$ | 30 | kg |
| $I_y$ | 830 | kg·m$^2$ |
| $I_x$ | 235 | kg·m$^2$ |
| $K_1$ $K_2$ | 20.6 | KN·m$^{-1}$ |
| $K_3$ $K_4$ | 15.2 | KN·m$^{-1}$ |
| $C_1$ $C_2$ | 1570 | N·s·m$^{-1}$ |
| $C_3$ $C_4$ | 1760 | N·s·m$^{-1}$ |
| $K_{t1}$ $K_{t2}$ | 138 | KN·m$^{-1}$ |
| $K_{t3}$ $K_{t4}$ | 138 | KN·m$^{-1}$ |
| $l_f$ $l_r$ | 1.36 | m |
| $l_a$ | 0.958 | m |
| $l_b$ | 1.377 | m |

*4.2. Simulation Module Design.* In order to validate the feasibility of the fuzzy increment controller, car suspension parameters are as given in Table 2.

Using MATLAB/Simulink, the simulation modular of active suspension with seven DOF is designed. According to formula (9) to formula (12), a road excitation simulation module of white noise in time-domain is designed as shown in Figure 4 taking into account the delay and correlation characteristic between the wheels. Here, the submodule of fuzzy increment controller in a wheel side is described as in Figure 5. The simulation submodule of the other three controllers is similar to Figure 5.

*4.3. Simulation Analysis.* Figures 6–8 show the acceleration's comparison results of the body vertical vibration, pitching, and rolling motion under the condition of white noise road surface excitation adopting different control modes.

As you can see from Figures 6–8, these indexes values on the vertical vibration, pitching, and rolling angular acceleration of the vehicle body have been improved adopting the Fuzzy-PID code compared to other modes under the condition of white noise road surface excitation. In other words, the fuzzy increment controller can obviously reduce the body's vibration because the acceleration peak amplitude above indexes is far less than other modes.

Figures 9–11 show the acceleration's comparison results of the body vertical vibration, pitching, and rolling motion under the condition of pulse excitation adopting different control mode.

From Figures 9–11 we can see that the vibration amplitude on vehicle body's acceleration is also far less than other modes adopting the Fuzzy-PID code under the condition of pulse excitation.

Figures 12–14 show the acceleration's comparison results of the body vertical vibration, pitching, and rolling motion under the condition of sinusoidal excitation adopting different control mode. As you can see from Figures 6–14, the fuzzy increment controller (i.e., the Fuzzy-PID code name) has good control effect in improving the body vertical vibration acceleration, pitching, and rolling angular acceleration comparing with the independent types of controls, such as the passive suspension, the PID control, and the fuzzy control.

In addition to comparison curves, the root mean square value of body's acceleration is counted regarding four kinds of

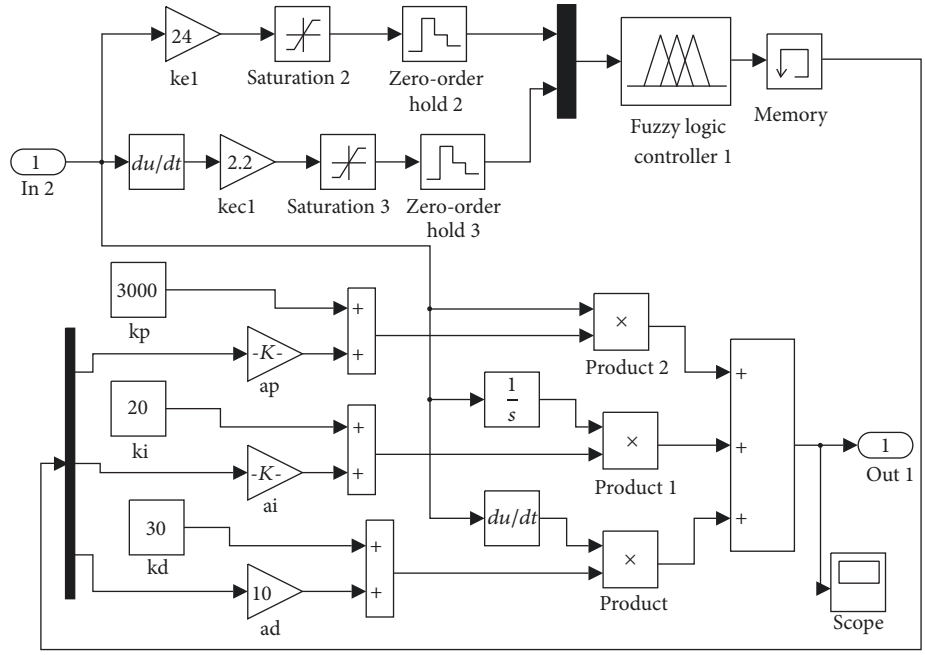


Figure 5: The submodule of fuzzy increment controller.

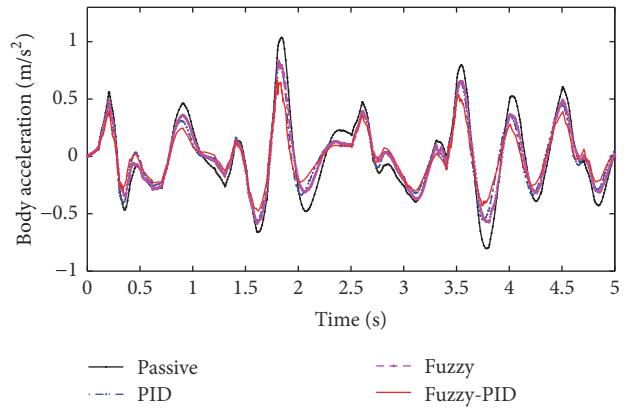


Figure 6: Comparison result of the body vertical vibration acceleration.

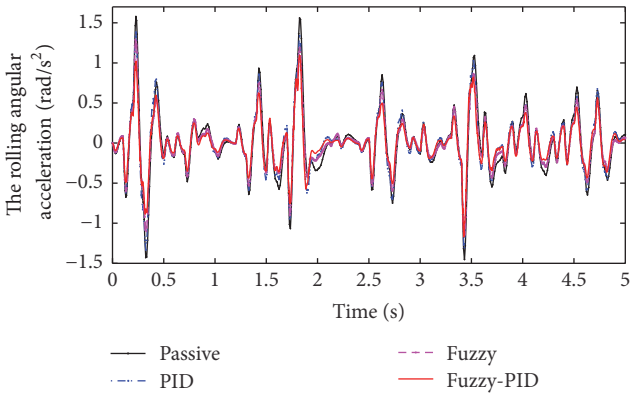


Figure 8: Comparison result of the body rolling angular acceleration.

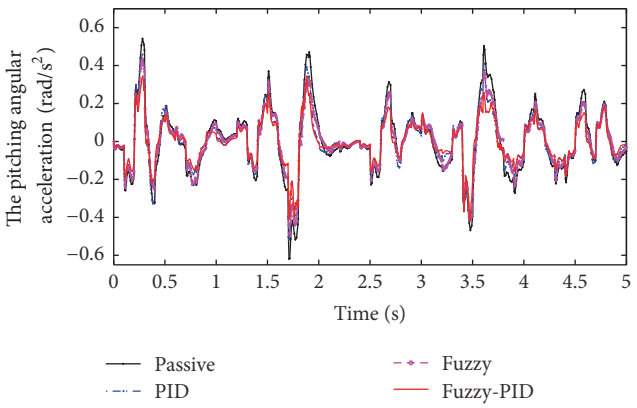


Figure 7: Comparison result of the body pitching angular acceleration.

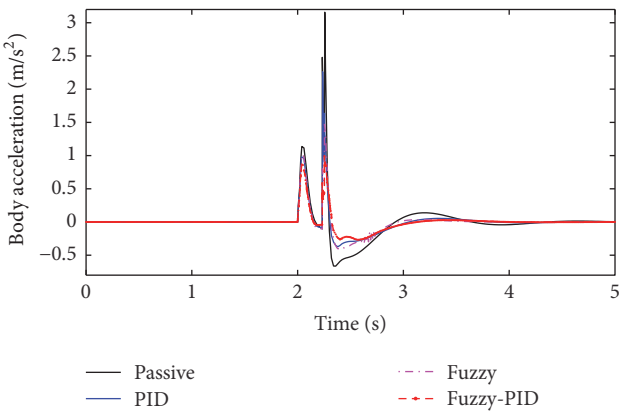


Figure 9: Comparison result of the body vertical vibration acceleration.

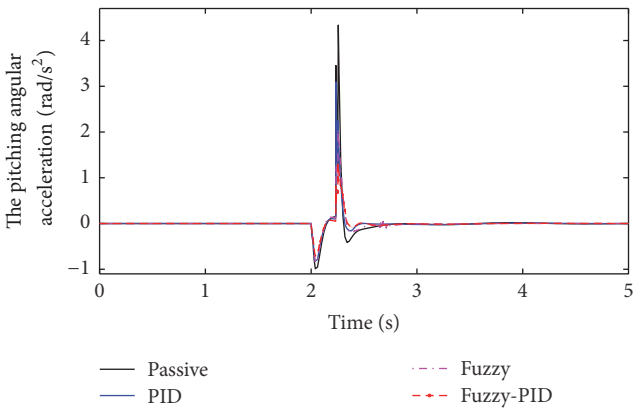


Figure 10: Comparison result of the pitching angular acceleration.

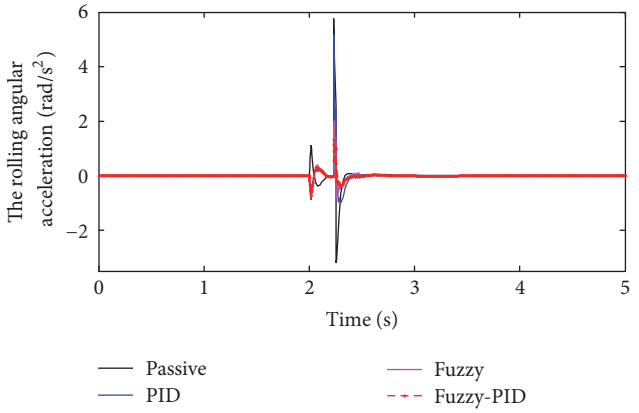


Figure 11: Comparison result of the body rolling angular acceleration.

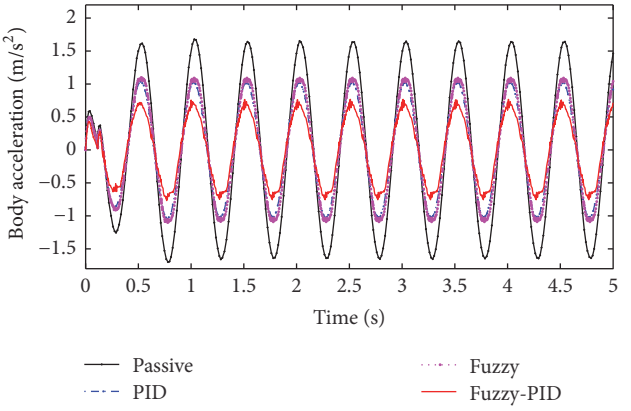


Figure 12: Comparison result of the vertical vibration acceleration.

control mode under the condition of different speed as shown in Table 3.

As seen from Table 3, the root mean square value of the body's acceleration, the pitching, and rolling angular acceleration adopting the Fuzzy-PID mode reduces 37.5 percent, 28.9 percent, and 26.2 percent compared with the passive mode under the condition of white noise road surface excitation. The root mean square values of indexes mentioned

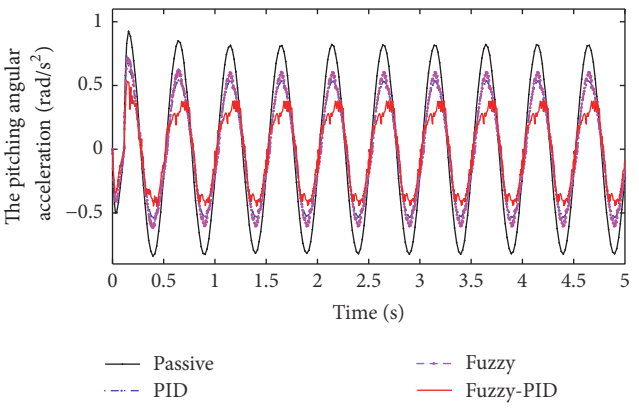


Figure 13: Comparison result of the pitching angular acceleration.

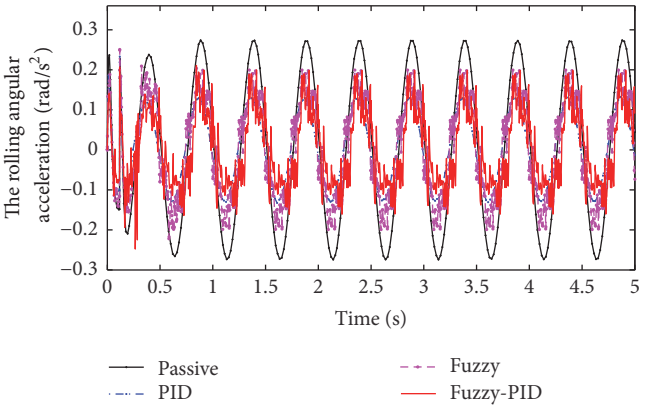


Figure 14: Comparison result of the rolling angular acceleration.

above reduce 56.2, 47.6, and 52.0 percent under the condition of sinusoidal excitation, respectively.

You can also see that the root mean square values of indexes mentioned above adopting the Fuzzy-PID mode have been improved obviously compared to other modes at 30 meters per second. Through analysis we can see that the designed controller can reduce obviously the vehicle vibration and has good control effect compared to the independent control type.

## 5. Conclusions

(1) The vibration model with seven degrees of freedom of automobile active suspension is derived and four fuzzy increment controllers are designed based on 49 rules for adapting the different real-time road input information.

(2) The white noise input model with four wheels correlated in characteristics of time-domain is designed that is closer to the actual road information input.

(3) Using MATLAB/Simulink, the simulation module of active suspension with seven DOF has been built and the fuzzy increment controller is validated taking the white noise excitation with four-wheel correlation in time-domain, the sinusoidal excitation, and the pulse excitation of C-grade road surface as the road input. The simulation results show

Table 3: The root mean square value of acceleration.

| Input | Speed | Control mode | Body vertical acceleration | Pitching angular acceleration | Rolling angular acceleration |
|---|---|---|---|---|---|
| White noise excitation | 20 m/s | Passive | 0.3800 | 0.2075 | 0.4937 |
| | | PID | 0.2862 | 0.1720 | 0.4462 |
| | | Fuzzy | 0.3031 | 0.1700 | 0.4237 |
| | | Fuzzy-PID | 0.2374 | 0.1475 | 0.3640 |
| | 30 m/s | Passive | 0.5383 | 0.2232 | 0.4247 |
| | | PID | 0.4205 | 0.1936 | 0.3828 |
| | | Fuzzy | 0.3987 | 0.1819 | 0.3217 |
| | | Fuzzy-PID | 0.3344 | 0.1673 | 0.2938 |
| The sinusoidal excitation | 20 m/s | Passive | 1.1386 | 0.5525 | 0.1858 |
| | | PID | 0.7232 | 0.3722 | 0.0938 |
| | | Fuzzy | 0.7950 | 0.3734 | 0.1159 |
| | | Fuzzy-PID | 0.4983 | 0.2891 | 0.0892 |
| | 30 m/s | Passive | 1.2356 | 0.2857 | 0.2111 |
| | | PID | 0.7881 | 0.2055 | 0.1111 |
| | | Fuzzy | 0.8587 | 0.2113 | 0.1225 |
| | | Fuzzy-PID | 0.6001 | 0.1653 | 0.1189 |

that designed fuzzy increment controller can reduce 37.5 percent, 28.9 percent, and 26.2 percent in evaluation index of the body vertical vibration acceleration, pitching, and rolling acceleration compared with the passive mode under the condition of white noise road surface excitation and can improve 56.2, 47.6, and 52.0 percent under the condition of sinusoidal excitation, respectively.

In a word, the designed fuzzy increment controller in this paper is feasible to adapt to real-time change of road situations and can reduce obviously the vehicle vibration and has a superior control effect compared to other control modes. The research achievements have much reference value for developing the product of suspension controller.

As future work, we intend to build the prototypes and develop products by single-chip technology.

## Conflicts of Interest

The authors declared no potential conflicts of interest with respect to the research, authorship, and/or publication of this article.

## Acknowledgments

This work was supported, in part, by the Natural Science Foundation of China under Grant 61473139 and the joint fund of the Natural Science Foundation of Liaoning Province of China 201602368.

## References

[1] H. Zhang, E. Wang, F. Min, R. Subash, and C. Su, "Skyhook-based semi-active control of full-vehicle suspension with magneto-rheological dampers," *Chinese Journal of Mechanical Engineering*, vol. 26, no. 3, pp. 498–505, 2013.

[2] H.-B. Ren, S.-Z. Chen, Y.-Z. Zhao, G. Liu, and L. Yang, "Observer-based hybrid control algorithm for semi-active suspension systems," *Journal of Central South University*, vol. 23, no. 9, pp. 2268–2275, 2016.

[3] D. Singh and M. L. Aggarwal, "Passenger seat vibration control of a semi-active quarter car system with hybrid fuzzy-PID approach," *International Journal of Dynamics and Control*, vol. 5, no. 2, pp. 287–296, 2017.

[4] H.-P. Du and N. Zhang, "Robust active suspension design subject to vehicle inertial parameter variations," *International Journal of Automation and Computing*, vol. 7, no. 4, pp. 419–427, 2010.

[5] Y.-J. Liu and S. Tong, "Adaptive fuzzy control for a class of unknown nonlinear dynamical systems," *Fuzzy Sets and Systems*, vol. 263, pp. 49–70, 2015.

[6] Y.-J. Liu, Y. Gao, S. Tong, and Y. Li, "Fuzzy approximation-based adaptive backstepping optimal control for a class of nonlinear discrete-time systems with dead-zone," *IEEE Transactions on Fuzzy Systems*, 1 page, 2015.

[7] Y. Gao and Y.-J. Liu, "Adaptive fuzzy optimal control using direct heuristic dynamic programming for chaotic discrete-time system," *Journal of Vibration and Control*, vol. 22, no. 2, pp. 595–603, 2016.

[8] H. Li, G. Chen, X. Liao, and T. Huang, "Leader-following consensus of discrete-time multiagent systems with encoding-decoding," *IEEE Transactions on Circuits and Systems II: Express Briefs*, vol. 63, no. 4, pp. 401–405, 2016.

[9] H. Li, C. Huang, G. Chen, X. Liao, and T. Huang, "Distributed Consensus Optimization in Multiagent Networks With Time-Varying Directed Topologies and Quantized Communication," *IEEE Transactions on Cybernetics*, 2017.

[10] C. Huang, L. Chen, H. Jiang, C. Yuan, and T. Xia, "Fuzzy chaos control for vehicle lateral dynamics based on active suspension system," *Chinese Journal of Mechanical Engineering*, vol. 27, no. 4, pp. 793–801, 2014.

[11] H. Li, S. Liu, Y. C. Soh, and L. Xie, "Event-Triggered Communication and Data Rate Constraint for Distributed Optimization of Multiagent Systems," *IEEE Transactions on Systems, Man, and Cybernetics: Systems*, pp. 1–12.

[12] H. Li, G. Chen, T. Huang, and Z. Dong, "High-performance consensus control in networked systems with limited bandwidth communication and time-varying directed topologies," *IEEE Transactions on Neural Networks and Learning Systems*, pp. 1–12, 2016.

[13] S. Riaz and L. Khan, "NeuroFuzzy Adaptive Control for Full-Car Nonlinear Active Suspension with Onboard Antilock Braking System," *Arabian Journal for Science and Engineering*, vol. 40, no. 12, pp. 3483–3505, 2015.

[14] M. M. Zirkohi and T.-C. Lin, "Interval type-2 fuzzy-neural network indirect adaptive sliding mode control for an active suspension system," *Nonlinear Dynamics*, vol. 79, no. 1, pp. 513–526, 2015.

[15] L. Balamurugan, J. Jancirani, and M. A. Eltantawie, "Generalized magnetorheological (MR) damper model and its application in semi-active control of vehicle suspension system," *International Journal of Automotive Technology*, vol. 15, no. 3, pp. 419–427, 2014.

[16] H. L. Zhang, E. R. Wang, N. Zhang, F. Min, R. Subash, and C. Su, "Semi-active sliding mode control of vehicle suspension with magneto-rheological damper," *Chinese Journal of Mechanical Engineering*, vol. 28, no. 1, pp. 63–75, 2015.

[17] S. Bououden, M. Chadli, L. Zhang, and T. Yang, "Constrained model predictive control for time-varying delay systems: Application to an active car suspension," *International Journal of Control, Automation, and Systems*, vol. 14, no. 1, pp. 51–58, 2016.

[18] L. Wu and W.-J. Zhang, "Hierarchical modeling of semi-active control of a full motorcycle suspension with six degrees of freedoms," *International Journal of Automotive Technology*, vol. 11, no. 1, pp. 27–32, 2010.

[19] Z. Mao, Y. Wang, B. Jiang, and G. Tao, "Fault diagnosis for a class of active suspension systems with dynamic actuators' faults," *International Journal of Control, Automation, and Systems*, vol. 14, no. 5, pp. 1160–1172, 2016.

[20] H. Trabelsi, P.-A. Yvars, J. Louati, and M. Haddar, "Evaluation of the effectiveness of the interval computation method to simulate the dynamic behavior of subdefinite system: application on an active suspension system," *International Journal on Interactive Design and Manufacturing*, vol. 9, no. 2, pp. 83–96, 2015.

[21] C. Wang, K. Deng, W. Zhao, G. Zhou, and X. Li, "Robust control for active suspension system under steering condition," *Science China Technological Sciences*, vol. 60, no. 2, pp. 199–208, 2017.

[22] X. Dong, D. Zhao, B. Yang, and C. Han, "Fractional-order control of active suspension actuator based on parallel adaptive clonal selection algorithm," *Journal of Mechanical Science and Technology*, vol. 30, no. 6, pp. 2769–2781, 2016.